HHS Public Access

Author manuscript

Mol Cancer Ther. Author manuscript; available in PMC 2015 May 04.

Published in final edited form as:

Mol Cancer Ther. 2008 May ; 7(5): 1080–1090. doi:10.1158/1535-7163.MCT-07-0526.

Reprogramming epigenetic silencing: artificial transcription factors synergize with chromatin remodeling drugs to reactivate the tumor suppressor *mammary serine protease inhibitor*

Adriana S. Beltran[1], **Xueguang Sun**[2], **Paul M. Lizardi**[2], and **Pilar Blancafort**[1]

[1]Department of Pharmacology and Lineberger Comprehensive Cancer Center, University of North Carolina at Chapel Hill, Chapel Hill, North Carolina

[2]Department of Biochemistry and Biophysics, Yale University Medical Center, New Haven, Connecticut

Abstract

Mammary serine protease inhibitor (*maspin*) is an important tumor suppressor gene whose expression is associated not only with tumor growth inhibition but also with decreased angiogenesis and metastasis. *Maspin* expression is down-regulated in metastatic tumors by epigenetic mechanisms, including aberrant promoter hypermethylation. We have constructed artificial transcription factors (ATFs) as novel therapeutic effectors able to bind 18-bp sites in the *maspin* promoter and reactivate *maspin* expression in cell lines that harbor an epigenetically silenced promoter. In this article, we have investigated the influence of epigenetic modifications on ATF-mediated regulation of *maspin* by challenging MDA-MB-231 breast cancer cells, comprising a methylated *maspin* promoter, with different doses of ATFs and chromatin remodeling drugs: the methyltransferase inhibitor 5-aza-2′-deoxycytidine and the histone deacetylase inhibitor suberoylanilide hydroxamic acid. We found that the ATFs synergized with both inhibitors in reactivating endogenous *maspin* expression. The strongest synergy was observed with the triple treatment ATF-126 + 5-aza-2′-deoxycytidine + suberoylanilide hydroxamic acid, in which the tumor suppressor was reactivated by 600-fold. Furthermore, this combination inhibited tumor cell proliferation by 95%. Our data suggest that ATFs enhance the efficiency of chromatin remodeling drugs in reactivating silenced tumor suppressors. Our results document the power of a novel therapeutic approach that combines both epigenetic and genetic (sequence-specific ATFs) strategies to reactivate specifically silenced regions of the genome and reprogram cellular phenotypes.

Introduction

Tumor suppressor genes play an essential role in controlling unscheduled cell proliferation and they act as gatekeepers that block neoplastic processes in tissues. Due to the pivotal role of tumor suppressor gene inactivation during tumor progression, these genes are primary

Requests for reprints: Pilar Blancafort, Department of Pharmacology and Lineberger Comprehensive Cancer Center, University of North Carolina at Chapel Hill, Chapel Hill, NC 27599-7365. Phone: 919-966-1614. pilar_blancafort@med.unc.edu.

targets in cancer therapeutics. Inactivation can occur via a variety of mechanisms, such as point mutations, deletions, and epigenetic modifications (1–3). Epigenetic modifications, such as DNA and histone methylation and histone deacetylation, result in a compact chromatin configuration that silences entire DNA regions (1–6). At the promoter level, this compact chromatin topology restricts the physical access of the polymerase II complex to regulatory sequence domains, resulting in inhibition of tumor suppressor transcription (7–9). Unlike genetic alterations, which irreversibly inactivate tumor suppression expression, epigenetic modifications are potentially reversible (9–11).

The reversible nature of epigenetic silencing offers a unique opportunity for therapeutic intervention by reactivating endogenous tumor suppressor genes. Several chromatin remodeling drugs have been developed to release the repressed state of tumor suppressor genes. These drugs act by inhibiting DNA methyltransferases or histone deacetylases (HDAC), resulting in increased promoter accessibility and enhanced tumor suppressor gene transcription (12 – 14). To date, the most widely used chromatin remodeling drug is the DNA methyltransferase inhibitor 5-aza-2′-deoxycytidine (5-aza-2′-dC), recently approved for therapeutic treatment (15). Several methyltransferase inhibitors [such as 5-aza-dC and MG98 (16, 17)] and HDAC inhibitors [such as suberoylanilide hydroxamic acid (SAHA; ref. 18), valproic acid (19), and pivaloyloxymethyl butyrate (20, 21)] are presently in phase I and II clinical trials. The small-molecule inhibitors 5-aza-2′-dC and SAHA have been used to reactivate tumor suppressor genes aberrantly methylated in aggressive tumor cells, such as *desmocollin 3* (22), *gelsolin* (23), and *mammary serine protease inhibitor* (*maspin*; refs. 13, 22). Moreover, several reports have shown that methyltransferase and HDAC inhibitors are able to synergize to reactivate tumor suppressor expression (24, 25). Nevertheless, potential limitations for the use of these drugs in cancer patients include their toxicity, lack of target specificity, and development of acquired drug resistance (6, 26). Thus, there is a need for the development of novel strategies to increase the targeted efficiency and specificity of current anticancer drugs.

Our laboratory has recently applied a new strategy to specifically reactivate tumor suppressor genes silenced by epigenetic mechanisms in aggressive tumors (27). We have targeted the tumor suppressor gene *maspin* using three rationally designed artificial transcription factors (ATFs). These ATFs comprise six sequence-specific zinc finger (ZF) domains, designed to recognize unique 18-bp sites in the *maspin* promoter. The ZFs were linked to the VP64 activator domain, which mediates promoter up-regulation. We found that the capability of the ATFs to up-regulate *maspin* depended on the cell line analyzed, indicating that the structure of the chromatin can influence ATF-mediated transactivation of *maspin*. In the aggressive MDA-MB-231 breast cancer cell line, which comprises a methylated and silenced *maspin* promoter, only one ATF (ATF-126) was able to partially reactivate the endogenous *maspin*. We hypothesized that the structure of the chromatin (which is found in a more compact configuration in methylated promoters) could act as a partial blockade and restrict ATF-mediated transactivation of *maspin*. In this article, we have investigated the influence of chromatin structure at the *maspin* promoter in the context of artificial ATF regulation by challenging MDA-MB-231 cells expressing ATF-126 with different doses of 5-aza-2′-dC and SAHA. We found that ATF synergized with both

inhibitors to reactivate *maspin* expression. The strongest synergy was observed with the triple treatment ATF-126 + 5-aza-2′-dC + SAHA, in which the tumor suppressor was reactivated by 600-fold. Furthermore, this combination inhibited breast tumor cell proliferation by 95%. Our data suggest that ATFs amplify the response of chromatin remodeling drugs in reactivating silenced tumor suppressors. Thus, combinations of low concentrations of chromatin remodeling drugs and sequence-specific ATFs are efficient in reactivating silenced regions of the genome and effectively reprogram cellular phenotypes. This could represent a powerful therapeutic strategy to target a variety of neoplasias through specific reactivation of tumor suppressor genes.

Materials and Methods

Cell Lines

MDA-MB-231 breast carcinoma, MDA-MB-468, MCF-12A, and 293TGagPol cell lines were obtained from the American Type Culture Collection.

Sodium Bisulfite Genomic Sequencing of the Maspin Promoter

Genomic DNA (1.5 μg) was modified with sodium bisulfite using EZ DNA Methylation-Gold kit (Zymo Research). The *maspin* promoter was amplified from the bisulfite-modified DNA by PCR using primers specific to the bisulfite-modified sequence of the maspin promoter: 5′-TAGGATTTTAAAAAGAAATTTTTTG-3′(forward primer) and 5′-CCCACCTTACTTACCTAAAATCACA-3′(reverse primer). The PCR products were cloned and 10 positive recombinants were sequenced. The methylation status of individual CpG sites was determined by comparison of the sequence obtained with the known maspin sequence.

ATF Retroviral Transduction

The retroviral vector pMX-6ZFs-VP64-IRES-GFP (28) was first cotransfected with a plasmid (pMDG.1) expressing the vesicular stomatitis virus envelope protein into 293TGag-Pol cells to produce retroviral particles. Transfection was done using Lipofectamine as recommended (Invitrogen). The viral supernatant was used to infect the host cell lines, and the infection efficiency was assessed by flow cytometry (FACSCalibur, BD Biosciences) using green fluorescent protein as marker.

Drug Treatments

ATF-transduced cells and control cells (0.25×10^6 untransduced cells, cells transduced with empty retroviral vector, and a control ATF that does not regulate *maspin*) were seeded in 10-cm tissue culture plates. These samples were treated with different concentrations of 5-aza-2′-dC (0, 0.025, 0.05, 0.125, 0.25, 0.625, 1.25, 2.5, 3.75, 6.25, 12.5, 25, 62.5, and 125 μg/mL; Sigma) or SAHA (0, 0.0133, 0.026, 0.066, 0.132, 0.26, 0.4, 0.66, 1.32, 2.6, 3.97, and 5.3 μg/mL; BioVision) or both inhibitors (5-aza-2′-dC and SAHA) during 48 h in a 37°C, 5% CO_2 incubator. Cells were collected, and the RNA was extracted, reverse transcribed, and processed for real-time quantification of *maspin*.

Real-time PCR Expression Assays

ATF-transduced cells and control cells, drug treated or nontreated, were collected, and the RNA was extracted and 2.5 μg were used for reverse transcription. Quantification of *maspin* and VP64 activator domain was obtained by real-time quantitative PCR using fluorescent Taqman assays (Applied Biosystems) as described (27). The primers and probes for the *VP64* activator domain were the following: 5′-AAGCGACGCATTGGATGAC-3′(forward primer), 5′-GGAACGTCGTACGGGTAGTTAATT3′(reverse primer), and 5′-6FAM-TCGGCTCCGATGCT-MGBNFQ-3′(probe). Real-time PCR data were analyzed using the comparative $2^{-\Delta\Delta CT}$ method (SDS 2.1 RQ software, Applied Biosystems) and results were expressed as "fold change" in *maspin* RNA expression normalized to *GAPDH* and relative to the vehicle-treated control (29).

Proliferation Assays

Proliferation assays were done measuring cell viability determined by a survival assay (XTT, Roche, according to the manufacturer's instructions). To measure the effect of ATF-126, 5-aza-2′-dC, and SAHA in cell viability, MDA-MB-231 breast cancer cells were transduced with different concentrations of ATF-126 plasmid or/and treated with 5-aza-2′-dC or SAHA (same concentration described earlier). Twenty-four hours after transfection, 3,000 cells per well (5 wells per concentration) were seeded into 96-well format tissue culture plates. Cell viability was measured using the XTT assay by monitoring the absorbance (405 nm) of the cells at 0 and 72 h after transduction and 48 h of drug treatment.

Experimental Drug Dose-Effect Plots

Dose-effect curves and median-effect plots were generated for each set of the real-time and proliferation data samples using the software package PharmToolsPro (McCary Group; ref. 30). The median-effect dose (Dm_{50}) and the slope (m) were calculated from the median-effect plots and introduced in the isobologram equation for the calculation of the CI (28, 31–33). The CI isobologram equation [$CI = (D)_1/(Dx)_1 + (D)_2/(Dx)_2 + (D)_3/(Dx)_3$] was used for data analysis of three-drug combination (31, 32). CI < 1, CI = 1, and CI > 1 indicate synergy, additive effect, and antagonism, respectively.

Statistical Analysis

Real-time PCR and viability experiments were repeated thrice using three independently processed samples. For each sample, we did triplicate acquisitions. Differences between all treatments were analyzed by the ANOVA test with a critical level of significance set up at $P < 0.05$, and significant differences between groups of treatments were analyzed with post hoc Turkish test using the software GraphPad Prism v.5.

Results

ATFs Reactivate *Maspin* in Combination with 5-Aza-2′-dC and SAHA

In a previous report, we have described the construction of three ATFs designed to bind 18-bp sites in the *maspin* proximal promoter (27). The ATFs were constructed by linkage of six sequence-specific ZF domains with the VP64 transactivator domain (Fig. 1A). Each ZF is a

compact 30-amino acid domain composed of a recognition α-helix packed with two antiparallel β-strands via the coordination of a zinc ion. The α-helix of each ZF specifically recognizes 3 bp in the DNA or "recognition triplet." The main contact positions are residue +6 of the recognition helix, which interacts with the 5′nucleotide position of the triplet, residue +3, interacting with the middle base, and position −1, which makes H-bonding contacts with the 3′nucleotide of the triplet (34).

Our previous results show that the efficiency of *maspin* activation by ATFs depended on the particular cell line analyzed, indicating that the structure of the chromatin may influence the ATF-mediated regulation of the endogenous promoter. To investigate the influence of promoter topology in ATF regulation, we focused our studies on the MDA-MB-231 cell line, an aggressive cell estrogen receptor–negative breast cancer cell line that comprises a methylated and silenced *maspin* promoter (35). First, we verified the methylation status of the *maspin* promoter in the MDA-MB-231 background by doing sodium bisulfate sequencing of the *maspin* proximal promoter and we mapped the ATF-binding sites in this sequence. As shown in Fig. 1B, the ATF-126–binding site contained two methylated cytosines, whereas the ATF-97–binding site comprised one methylated cytosine. In contrast, both ATF-452–binding and the two p53-binding sites in the *maspin* promoter mapped in methylation-free regions. The same methylation pattern was found in other aggressive cancer cell lines comprising a silenced *maspin* promoter (data not shown). The ATF-binding sites were not found mutated or deleted in all 10 genomic clones processed by sequencing. This agrees with previous reports (35–37), which showed that *maspin* gene is not found mutated or deleted in tumor cells, but its promoter is silenced by epigenetic mechanisms. Consistent with this epigenetic silencing, we found that MDA-MB-231 cells have no detectable maspin protein as assessed by Western blotting (Fig. 2C). When retrovirally transduced in MDA-MB-231 cells, only the ATF-126 was able to strongly reactivate the promoter (70-fold relative to controls, in the absence of drugs), whereas ATF-97 and ATF-452 alone had a much weaker activity (27).

To investigate the influence of methylation and chromatin structure on ATF regulation, we challenged ATF-expressing cells with 5-aza-2′-dC and SAHA (Fig. 2). These drugs are known to induce a more relaxed promoter topology, which facilitates the access of transcription factors and DNA polymerase complex (7, 8, 38). 5-Aza-2′-dC causes inhibition of DNA methyltransferase activity. The DNA methyltransferase is bound irreversible to the DNA through the 5-aza-2′-dC residues, which results in a depletion of soluble DNA methyltransferase protein levels. The lack of DNA methyltransferase availability leads to a DNA replication with global demethylation (22, 39–41). SAHA interacts with HDAC enzymes at the catalytic site inhibiting their activity. This process leads to histone acetylation, which opens the chromatin structure, increasing transcriptional activity (42, 43). We hypothesized that remodeling the chromatin in the MDA-MB-231 cell line toward a more open configuration facilitated by 5-aza-2′-dC or/and SAHA enhances the efficiency of ATF regulation of *maspin.* To test this hypothesis, we first retrovirally transduced ATF-97, ATF-126, and ATF-452 into MDA-MB-231 cells. Additionally, cells were transduced with a control empty retroviral vector (control) and with a retroviral vector lacking the ZF domains (pMXVP64SS). These samples were treated with 5-aza-2′-dC (5 μg/mL) or SAHA

(0.5 μg/mL) or both inhibitors (5 and 0.5 μg/mL) and processed by real-time PCR for quantification of *maspin* mRNA levels. These concentrations were chosen in the range of the median-effect dose [Dm_{50}, the concentration of inhibitor giving rise to 50% of maximum maspin mRNA up-regulation (31, 32, 44) calculated for these drugs (Fig. 3A–C)]. *Maspin* mRNA levels were calculated as a "fold change in mRNA expression" relative to the vehicle-treated MDA-MB-231 cell line as explained in Materials and Methods. Previously, we have found that in the absence of inhibitor only ATF-126 was able to strongly up-regulate *maspin* compared with control cells (cells transduced with an empty retroviral vector), whereas ATF-97 and ATF-452 had a much weaker effect (27). To compare differences between treatments and to evaluate synergisms, we used an ANOVA test with a critical level of significance set up at $P < 0.05$. Significant differences between groups of treatments were analyzed with post hoc Turkish test.

As shown in Fig. 2A, particular ATFs synergized with chromatin remodeling drugs in reactivating *maspin* expression. ATF-452, which had a poor activity in up-regulating the promoter (3.2-fold), was not able to synergize with 5-aza-2′-dC, SAHA, or both inhibitions in up-regulating *maspin* expression. ATF-97 up-regulated *maspin* by 14-fold and synergized with both inhibitors when used separately: 5-aza-2′-dC (63-fold *maspin* up-regulation) and SAHA (156-fold). However, the triple treatment ATF-126 + 5-aza-2′-dC + SAHA did not significantly further improved regulation. ATF-126–transduced cells up-regulated *maspin* by 70-fold. This ATF synergized with both inhibitors, 5-aza-2′-dC (161-fold) and SAHA (376-fold), in reactivating maspin. In contrast with the other ATFs, the triple treatment ATF-126 + 5-aza-2′-dC + SAHA exhibited synergy, up-regulating *maspin* mRNA levels by 600-fold. This stimulatory effect leads to an 8.26-fold change in *maspin* mRNA expression relative to a breast cancer cell line carrying a nonmethylated promoter (the MDA-MB-468 cell line) and to ~40% of the expression levels observed in nontransformed breast epithelial cell lines, such as MCF-12A (Fig. 2B and C). In contrast with breast cancer cells, nontransformed breast epithelial cells express very high levels of *maspin* (37). Our data suggest that other epigenetic marks, in addition to methylation and histone acetylation, might contribute to maspin silencing in tumor cells.

Because the three ATFs target distinct 18-bp sites along the *maspin* promoter, their particular responses to the inhibitors could reflect local differences in methylation and/or acetylation levels in the chromatin. Overall, these experiments suggested that modifications of the chromatin leading to a more compact promoter topology could partially block or impair ATF regulation, probably by affecting ATF binding.

ATF-126 Synergizes with Low Concentrations of 5-Aza-2′dC and SAHA in Reactivating Maspin Expression

We subsequently focused our studies on ATF-126 because among all the ATFs analyzed it exhibited the strongest response in reactivating *maspin* in combination with chromatin remodeling drugs. High concentration or persistent exposure of tumor cells with chromatin remodeling drugs can potentially result in high toxicity (38, 45). Thus, novel approaches to reactivate tumor suppression expression while minimizing the exposure of tumor cells to the drugs are desired. We next investigated if synergy between the ATF and the chromatin

remodeling drugs was maintained when low concentrations of inhibitors (below their Dm_{50}) were used. The Dm_{50} was calculated for each treatment, 5-aza-2′-dC, SAHA, and ATF-126, using dose-effect plots in the MDA-MB-231 breast cancer cell line (Fig. 3A–D). In these experiments, MDA-MB-231 cells were treated with different concentrations of 5-aza-2′-dC (0.025–125 μg/mL; Fig. 3A) or SAHA (0.07–5.3 μg/mL; Fig. 3B) during 48 h and *maspin* mRNA expression levels were monitored by real-time PCR assays. For ATF-126, cells were transduced with increasing concentrations of ATF-encoded DNA (0–1.3 μg/mL; Fig. 3C), and 72 h after transduction, cells were processed by real-time PCR to detect ATF-126 and *maspin* mRNA levels. The concentration of ATF-126 DNA used in the transfection correlated with ATF-126 mRNA levels detected in MDA-MB-231–transduced cells, as assessed by real-time PCR using ATF-specific primers (Fig. 3D). ATF-126 reactivated *maspin* in a concentration-dependent manner, reaching a maximum effect of 300-fold *maspin* mRNA relative to control cells, whereas 5-aza-2′-dC and SAHA induced a maximum of 13-fold *maspin* up-regulation relative to control cells. The dose-response plots were used to calculate the Dm_{50} for each single treatment. For ATF-126, the Dm_{50} (0.525 μg/mL) was calculated as 50% *maspin* up-regulation at 72 h after transduction. For the inhibitors, the Dm_{50} was calculated as 50% *maspin* up-regulation after 48 h of drug treatment, being 5.55 and 0.75 μg/mL for 5-aza-2′dC and SAHA, respectively (Fig. 3A and B).

To study the synergy between ATF-126 and the chromatin remodeling drugs in reactivating *maspin*, we designed different drug combination experiments where the ATF-126 was used at its Dm_{50} and the inhibitors were used at their respective Dm_{50} (combination 1), $_{1/2}Dm_{50}$ (combination 2), and $_{1/3}Dm_{50}$ (combination 3; Fig. 3F). As a control, MDA-MB-231 cells were subjected to single treatments (transduced with ATF-126 for 72 h or exposed to 5-aza-2′-dC or SAHA for 48 h) and processed by real-time PCR to evaluate *maspin* mRNA levels. We additionally evaluated *maspin* mRNA levels for double and triple treatments using specific combinations of control cells, ATF-126–transduced cells, 5-aza-2′-dC, and SAHA (Fig. 3E). In all the combinations tested, we found that ATF-126 was able to synergize with 5-aza-2′-dC, SAHA, and both inhibitors to reactivate *maspin*. We found that the most effective combination in activating *maspin* was the triple treatment ATF-126 + 5-aza-2′-dC + SAHA, with a 600-fold *maspin* up-regulation, when all the compounds were combined at their Dm_{50} (drug combination 1). Furthermore, ATF-126 synergized with 5-aza-2′-dC and SAHA in reactivating *maspin* expression by 413-fold even using $_{1/3}Dm_{50}$ of inhibitors (drug combination 3). No statistical difference was observed between combination 2 (when 5-aza-2′-dC and SAHA were used at their $_{1/2}Dm_{50}$) and combination 3 (when 5-aza-2′-dC and SAHA were used at their $_{1/3}Dm_{50}$). Overall, these results indicate that ATF-126 strongly synergized with a combination of methyltransferase and HDAC inhibitors to reactivate *maspin* expression and this synergism was maintained when low concentrations of inhibitors (below their Dm_{50}) were used.

ATF-126 Synergizes with 5-Aza-2′dC and SAHA to Inhibit Tumor Cell Viability

Several reports showed that induction of *maspin* mRNA expression results in inhibition of tumor cell proliferation by enhancement of apoptosis. We next investigated if ATF-126 could also synergize with 5-aza-2′-dC and SAHA in inducing inhibition of tumor cell

growth. MDA-MB-231 cells were transduced with a control vector or with ATF-126, and 72 h after transduction, these cells were treated with 5-aza-2′-dC, SAHA, or both inhibitors during 48 h. Tumor cell viability was evaluated using survival assays {2,3-bis[2-methoxy-4-nitro-5-sulfophenyl]-2H-tetrazolium-5-carboxanilide inner salt (XTT) assays}. The dose-effect plots for ATF-126, 5-aza-2′-dC, and SAHA (Fig. 4A) were used to calculate the inhibitory concentration (IC_{50}, the concentration of ATF-126 or inhibitor giving rise to 50% of inhibition of tumor cell growth at 72 h after transduction or after 48 h of drug treatment). The IC_{50} values were 0.15, 2.056, and 0.942 μg/mL for ATF-126, 5-aza-2′-dC, and SAHA, respectively. To evaluate synergisms, we applied a standard combinatorial method, which uses the isobologram equation to calculate the combinatorial index (CI). The interaction between drugs is defined as synergistic if CI < 1, antagonistic if CI > 1, and additive if CI = 1 (Fig. 4B). Control-transduced or ATF-126–transduced cells were challenged with different concentrations of 5-aza-2′-dC, SAHA, or both inhibitors, as shown in Table 1. We used concentrations of ATF/5-aza-2′-dC/SAHA in the range of the IC_{50} value, which resulted on 30% to 80% of tumor cell growth inhibition. As shown in Fig. 4B, ATF-126 synergized with 5-aza-2′-dC, SAHA, and both inhibitors (5-aza-2′-dC + SAHA) for the majority of the drug combinations tested. The synergistic effect for the double treatments ATF-126 + 5-aza-2′-dC, ATF-126 + SAHA, and 5-aza-2′-dC + SAHA was higher when low concentrations were used in each combination. For the triple treatment ATF-126 + 5-aza-2′-dC + SAHA, we observed a synergistic effect with all the combinations tested. The lowest (most synergistic) CI was achieved by the combination with the highest dose of ATF-126 and inhibitors, which results in 95% of inhibition of tumor cell viability compared with vehicle-treated control cells (Fig. 4C; doses are indicated in Table 1).

As shown in Fig. 4C, the triple treatment ATF-126 + 5-aza-2′-dC + SAHA was significantly the most efficient in decreasing tumor cell viability compared with all the other treatments. The double combinations ATF-126 + SAHA and ATF-126 + 5-aza-2′-dC reduced significantly cell viability compared with all the single treatments (ATF-126, 5-aza-2′-dC, and SAHA and vehicle; $P = 0.05$). However, our data in Fig. 4C did not reveal statistical differences between the following treatments: SAHA, 5-aza-2′-dC + SAHA, and ATF-126. The apparent discrepancy between the RNA and the viability data could be explained by the fact that these experiments measure different outcomes. Unlike real-time, which specifically measures *maspin* mRNA levels, cell viability is a complex phenotype involving many different gene products, including tumor suppressors such as *maspin*. The higher effect of SAHA and 5-aza-2′-dC observed in viability assays might suggest that these compounds reactivate many tumor suppressor genes, not just *maspin* (46, 47). Although off-target effects are possible with ATFs, these proteins have been engineered to reactivate specifically *maspin* and are not expected to regulate other tumor suppressor genes. We are presently investigating putative off-target effects of ATF-126.

To verify that the effect of the ATFs and inhibitors was specific for tumor cells and not normal epithelial cells, we did the same viability assays in a nontransformed breast epithelial cell line, the MCF-12A. In contrast with the MDA-MB-231 cell line, none of the combinations of ATFs and inhibitor was able to significantly up-regulate *maspin* expression

nor decrease cell viability as assessed by the ANOVA and post hoc Turkish tests (Supplementary Fig. S1).[3]

Discussion

In this article, we have investigated the influence of promoter structure in the regulation of the tumor suppressor gene *maspin* by ATFs. We have focused our analysis on the highly invasive, metastatic breast cancer cell line MDA-MB-231, which comprises a *maspin* promoter silenced by methylation and transcriptional repression (35), and on ATF-126, the strongest maspin regulator in this cell line (27). We have challenged MDA-MB-231 cells expressing ATF-126 with different doses of the methyltransferase inhibitor 5-aza-2′-dC and the HDAC1 inhibitor SAHA. These drugs interfere with repressive mechanisms, which maintain inaccessible chromatin structure: aberrant cytosine methylation and recruitment of HDAC complexes. Consequently, these inhibitors are able to relax the chromatin, facilitating access to the polymerase II transcriptional machinery (7 – 9). We hypothesized that disruption of the epigenetic silencing mediated by methyltransferase and HDAC inhibitors coupled to ATFs would result in an enhanced up-regulation of silenced genes. Our work shows that ATFs synergized with chromatin remodeling drugs to reactivate endogenous *maspin* expression. We found that *maspin* reactivation in response to the inhibitors depended on the ATF-binding site analyzed. It could be that, in the endogenous gene, these sites map in regions of the promoter that contain different levels of histone/methylcytosine modifications. It is also possible that other endogenous factors, such as additional epigenetic marks in the nucleosome, the positioning of the nucleosomes, and CpG-binding proteins, could affect ATF binding and regulation. The strongest synergy was observed with a triple treatment (ATF-126 + 5-aza-2′-dC + SAHA), in which the tumor suppression was reactivated by 600-fold. Consistent with the tumor-suppressive functions of *maspin*, we found that this triple drug combination was also the most effective in inhibiting breast tumor cell proliferation *in vitro*.

A plausible model explaining this synergy is shown in Fig. 5. In a context of a silenced promoter, methylated CpG islands are associated with methyl-binding proteins, methyltransferases, and HDAC, which maintain the promoter in a compact configuration, inaccessible to the transcriptional machinery (4–6). Likewise, it is possible that in the context of a repressed *maspin* promoter the ATF-binding sites are not optimally accessible to the ATFs. In the ATF, the ZF domains are linked to the strong transactivator domain VP64, which recruits the mediator protein and other polymerase II–associated proteins (including chromatin remodeling enzymes and histone acetyltransferases), resulting in a partial *maspin* reactivation. The synergy between the ATF and the chromatin remodeling drugs could be explained by drug-induced enhanced accessibility of the ATFs for their target sites in the *maspin* promoter.

Methyltransferase and HDAC inhibitors interfere with two enzymatic mechanisms of repression: 5-aza-2′-dC inhibits DNA methyltransferase Dnmt1 enzyme (39, 41, 49), whereas SAHA promotes histone acetylation and weakens the histone-DNA interactions

[3]Supplementary material for this article is available at Molecular Cancer Therapeutics (http://mct.aacrjournals.org/).

(50). Synergy between methyltransferase and HDAC agents in reactivating silenced tumor suppressors has been previously reported by many groups (14, 22, 25, 51, 52). Our results further show that ATF expression highly amplifies the gene reactivation effect of chromatin remodeling drugs with different mechanisms of action. In contrast with chromatin remodeling drugs, which potentially alter many genes in the genome, the ATF is used as a sequence-specific regulator of tumor suppression expression. Our results agree with a report showing that overexpression of the p53 transcription factor in the p53-deficient MDA-MB-231 cell line leads to a synergy with 5-aza-2′-dC in reactivation of the tumor suppressor *maspin* (13). We have found that, like natural transcription factors, ATFs can strongly synergize with both methyltransferase and HDAC inhibitors. Because ATFs can be designed for virtually any sequence in the human genome, the strategy presented in this article can be potentially applied for the reactivation of any epigenetically silenced promoter. Current ATF technology can generate ATF binding designed sequences with high specificity and selectivity in both *in vitro* binding assays and in reporter transactivation assays. Only a subset of ATFs designed against a given target promoter results in successful endogenous regulation (27), indicating that subtle aspects of the architecture of endogenous promoters may be key determinants for ATF-mediated regulation. Chromatin modifications could limit the binding of the ATFs *in vivo* by restricting ATF target site accessibility. This idea is supported by our observations, which show a gain of ATF-mediated regulation of silenced promoters only in the presence of chromatin remodeling drugs with ATFs having poor or no activity in the absence of remodeling-inducing compounds.

Importantly, we found that strong synergy between ATF/chromatin remodeling drugs was maintained in a concentration range of inhibitors below their IC_{50}. Although more experiments need to be done to evaluate the applicability of our findings to experiments using tumor models *in vivo*, our work shows proof of concept of an exciting strategic approach in therapeutics, which uses ATFs to amplify the apoptotic response of anticancer agents with locus-targeted gene activation while minimizing the exposure/concentration of the drugs.

Acknowledgments

We thank Dr. Lee Graves for the critical reading of the manuscript.

Grant support: NIH/National Cancer Institute grant 1R01CA125273-01, American Lung Association and LUNGevity Foundation grant LD-17098-N, V-Foundation Award, and Department of Defense Idea Award BC051475 (P. Blancafort) and National Cancer Institute grant 1 R21 CA116079-01 (P.M. Lizardi).

References

1. Jones PA, Laird PW. Cancer epigenetics comes of age. Nat Genet. 1999; 2:163–8. [PubMed: 9988266]
2. Baylin SB, Herman JG. DNA hypermethylation in tumorigenesis: epigenetics joins genetics. Trends Genet. 2000; 4:168–74. [PubMed: 10729832]
3. Bourdon JC. p53 and its isoforms in cancer. Br J Cancer. 2007; 3:277–82. [PubMed: 17637683]
4. Szyf M, Pakneshan P, Rabbani SA. DNA methylation and breast cancer. Biochem Pharmacol. 2004; 6:1187–97. [PubMed: 15313416]
5. Ting AH, McGarvey KM, Baylin SB. The cancer epigenome—components and functional correlates. Genes Dev. 2006; 20:3215–31. [PubMed: 17158741]

6. Jones PA, Baylin SB. The epigenomics of cancer. Cell. 2007; 128:683–92. [PubMed: 17320506]
7. Collingwood TN, Urnov FD, Wolffe AP. Nuclear receptors: coactivators, corepressors and chromatin remodeling in the control of transcription. J Mol Endocrinol. 1999; 3:255–75. [PubMed: 10601972]
8. Ohm JE, McGarvey KM, Yu X, et al. A stem cell-like chromatin pattern may predispose tumor suppressor genes to DNA hypermethylation and heritable silencing. Nat Genet. 2007; 39:237–42. [PubMed: 17211412]
9. Baylin SB. DNA methylation and gene silencing in cancer. Nat Clin Pract Oncol. 2005; 1:S4–11. [PubMed: 16341240]
10. Bastian PJ, Yegnasubramanian S, Palapattu GS, et al. Molecular biomarker in prostate cancer: the role of CpG island hypermethylation. Eur Urol. 2004; 6:698–708. [PubMed: 15548435]
11. Nuyt AM, Szyf M. Developmental programming through epigenetic changes. Circ Res. 2007; 4:452–5. [PubMed: 17332436]
12. Cameron EE, Bachman KE, Myohanen S, Herman JG, Baylin SB. Synergy of demethylation and histone deacetylase inhibition in the re-expression of genes silenced in cancer. Nat Genet. 1999; 1:103–7. [PubMed: 9916800]
13. Oshiro MM, Watts GS, Wozniak RJ, et al. Mutant p53 and aberrant cytosine methylation cooperate to silence gene expression. Oncogene. 2003; 22:3624–34. [PubMed: 12789271]
14. Hellebrekers DM, Griffioen AW, van Engeland M. Dual targeting of epigenetic therapy in cancer. Biochim Biophys Acta. 2007; 1:76–91. [PubMed: 16930846]
15. Samlowski WE, Leachman SA, Wade M, et al. Evaluation of a 7-day continuous intravenous infusion of decitabine: inhibition of promoter-specific and global genomic DNA methylation. J Clin Oncol. 2005; 17:3897. [PubMed: 15753459]
16. Winquist E, Knox J, Ayoub JP, et al. Phase II trial of DNA methyltransferase 1 inhibition with the antisense oligonucleotide MG98 in patients with metastatic renal carcinoma: a National Cancer Institute of Canada Clinical Trials Group investigational new drug study. Invest New Drugs. 2006; 2:159–67. [PubMed: 16502349]
17. Lyko F, Brown R. DNA methyltransferase inhibitors and the development of epigenetic cancer therapies. J Natl Cancer Inst. 2005; 20:1498–506. [PubMed: 16234563]
18. Laird PW. Cancer epigenetics. Hum Mol Genet. 2005; 1:65–76.
19. Münster P, Marchion D, Bicaku E, et al. Phase I trial of histone deacetylase inhibition by valproic acid followed by the topoisomerase II inhibitor epirubicin in advanced solid tumors: a clinical and translational study. J Clin Oncol. 2007; 15:1979–85. [PubMed: 17513804]
20. Patnaik A, Rowinsky EK, Villalona MA. A phase I study of pivaloyloxymethyl butyrate, a prodrug of the differentiating agent butyric acid, in patients with advanced solid malignancies. Clin Cancer Res. 2002; 7:2142–8. [PubMed: 12114414]
21. Reid T, Valone F, Lipera W, et al. Phase II trial of the histone deacetylase inhibitor pivaloyloxymethyl butyrate (Pivanex, AN-9) in advanced non-small cell lung cancer. Lung Cancer. 2004; 3:381–6. [PubMed: 15301879]
22. Wozniak RJ, Klimecki WT, Lau SS, Feinstein Y, Futscher BW. 5-Aza-2′-deoxycytidine-mediated reductions in G9A histone methyltransferase and histone H3 dimethylation levels are linked to tumor suppressor gene reactivation. Oncogene. 2007; 1:77–90. [PubMed: 16799634]
23. Primeau M, Gagnon J, Momparler RL. Synergistic antineoplastic action of DNA methylation inhibitor 5-AZA-2′-deoxycytidine and histone deacetylase inhibitor depsipeptide on human breast carcinoma cells. Int J Cancer. 2003; 2:177–84. [PubMed: 12455031]
24. Zhu WG, Otterson GA. The interaction of histone deacetylase inhibitors and DNA methyltransferase inhibitors in the treatment of human cancer cells. Curr Med Chem Anti-Canc Agents. 2003; 3:187–99.
25. Hurtubise A, Momparler RL. Effect of histone deacetylase inhibitor LAQ824 on antineoplastic action of 5-aza-2′-deoxycytidine (decitabine) on human breast carcinoma cells. Cancer Chemother Pharmacol. 2006; 5:618–25. [PubMed: 16783580]
26. Juttermann R, Li E, Jaenisch R. Toxicity of 5-aza-2′-deoxycytidine to mammalian cells is mediated primarily by covalent trapping of DNA methyltransferase rather than DNA demethylation. Proc Natl Acad Sci U S A. 1994; 25:11797–801. [PubMed: 7527544]

27. Beltran A, Parikh S, Liu Y, et al. Re-activation of a dormant tumor suppressor gene maspin by designed transcription factors. Oncogene. 2007; 19:2791–8. [PubMed: 17057734]
28. Blancafort P, Magnenat L, Barbas CF III. Scanning the human genome with combinatorial transcription factor libraries. Nat Biotechnol. 2003; 21:269–74. [PubMed: 12592412]
29. Livak KJ, Schmittgen TD. Analysis of relative gene expression data using real-time quantitative PCR and the 2(−ΔΔ*C*(T)) method. Methods. 2001; 4:402–8. [PubMed: 11846609]
30. Tallarida, RJ. Drug synergism and dose-effect data analysis. Florida: CRC Press; 2000. p. 15-71.
31. Chou TC, Talalay P. Quantitative analysis of dose-effect relationships: the combined effects of multiple drugs or enzyme inhibitors. Adv Enzyme Regul. 1984; 22:27–55. [PubMed: 6382953]
32. Chou TC. Assessment of synergistic and antagonistic effects of chemotherapeutic agents *in vitro*. Contrib Gynecol Obstet. 1994; 19:91–107. [PubMed: 7995057]
33. Berenbaum MC. What is synergy? Pharmacol Rev. 1989; 2:93–141. [PubMed: 2692037]
34. Pavletich NP, Pabo CO. Zinc finger-DNA recognition: crystal structure of a Zif268-DNA complex at 2. 1 A. Science. 1991; 252:809–17. [PubMed: 2028256]
35. Futscher BW, Oshiro MM, Wozniak RJ, et al. Role for DNA methylation in the control of cell type specific maspin expression. Nat Med. 2002; 31:175–9.
36. Zou Z, Anisowicz A, Hendrix MJ, et al. Maspin, a serpin with tumor-suppressing activity in human mammary epithelial cells. Science. 1994; 5146:526–9. [PubMed: 8290962]
37. Domann FE, Rice JC, Hendrix MJC, Futscher BW. Epigenetic silencing of maspin gene expression in human breast cancers. Int J Cancer. 2000; 85:805–10. [PubMed: 10709100]
38. Baylin SB, Schuebel KE. Genomic biology: the epigenomic era opens. Nature. 2007; 7153:553–60.
39. Creusot F, Acs G, Christman JK. Inhibition of DNA methyltransferase and induction of Friend erythroleukemia cell differentiation by 5-azacytidine and 5-aza-2′-deoxycytidine. J Biol Chem. 1982; 4:2041–8. [PubMed: 6173384]
40. Cheng JC, Yoo CB, Weisenberger DJ, et al. Preferential response of cancer cells to zebularine. Cancer Cell. 2004; 2:151–8. [PubMed: 15324698]
41. Palii SS, Van Emburgh BO, Sankpal UT, Brown KD, Robertson KD. The DNA methylation inhibitor 5-aza-2′-deoxycytidine induces reversible genome-wide DNA damage that is distinctly influenced by DNA methyl-transferases 1 and 3B. Mol Cell Biol. 2008; 28:752–71. [PubMed: 17991895]
42. Marks PA, Richon VM, Rifkind RA. Histone deacetylase inhibitors: inducers of differentiation or apoptosis of transformed cells. J Natl Cancer Inst. 2000; 15:1210–6. [PubMed: 10922406]
43. Marks PA, Breslow R. Dimethyl sulfoxide to vorinostat: development of this histone deacetylase inhibitor as an anticancer drug. Nat Biotechnol. 2007; 1:84–90. [PubMed: 17211407]
44. Chou TC. Theoretical basis, experimental design, and computerized simulation of synergism and antagonism in drug combination studies. Pharmacol Rev. 2006; 3:621–81. [PubMed: 16968952]
45. Brock MV, Herman JG, Baylin SB. Cancer as a manifestation of aberrant chromatin structure. Cancer J. 2007; 1:3–8. [PubMed: 17464240]
46. Desmond JC, Raynaud j, Tung E, et al. Discovery of epigenetically silenced genes in acute myeloid leukemias. Leukemia. 2007; 21:1026–34. [PubMed: 17330099]
47. Kumagai T, Wakimoto N, Yin D, et al. Histone deacetylase inhibitor, suberoylanilide hydroxamic acid (vorinostat, SAHA) profoundly inhibits the growth of human pancreatic cancer cells. Int J Cancer. 2007; 3:656–65. [PubMed: 17417771]
48. Gui CY, Ngo L, Xu WS, Richon VM, Marks PA. Histone deacetylase (HDAC) inhibitor activation of p21WAF1 involves changes in promoter-associated proteins, including HDAC1. Proc Natl Acad Sci U S A. 2004; 5:1241–6. [PubMed: 14734806]
49. Christman JK. 5-Azacytidine and 5-aza-2′-deoxycytidine as inhibitors of DNA methylation: mechanistic studies and their implications for cancer therapy. Oncogene. 2002; 35:5483–95. [PubMed: 12154409]
50. Rundall BK, Denlinger CE, Jones DR. Suberoylanilide hydroxamic acid combined with gemcitabine enhances apoptosis in non-small cell lung cancer. Surgery. 2005; 2:360–7. [PubMed: 16153448]

51. Shaker S, Bernstein M, Momparler LF, Momparler RL. Preclinical evaluation of antineoplastic activity of inhibitors of DNA methylation (5-aza-2′-deoxycytidine) and histone deacetylation (trichostatin A, depsipeptide) in combination against myeloid leukemic cells. Leuk Res. 2005; 5:437–44.

52. Becker JC, Ugurel S, Bröcker EB, Schrama D, Houben R. New therapeutic approaches for solid tumors: histone deacetylase, methyltransferase and proteasome inhibitors. J Dtsch Dermatol Ges. 2006; 2:108–13. [PubMed: 16503937]

53. Zhang M, Magit D, Sager R. Expression of maspin in prostate cells is regulated by a positive ets element and a negative hormonal responsive element site recognized by the androgen receptor. Proc Natl Acad Sci U S A. 1997; 94:5673–8. [PubMed: 9159131]

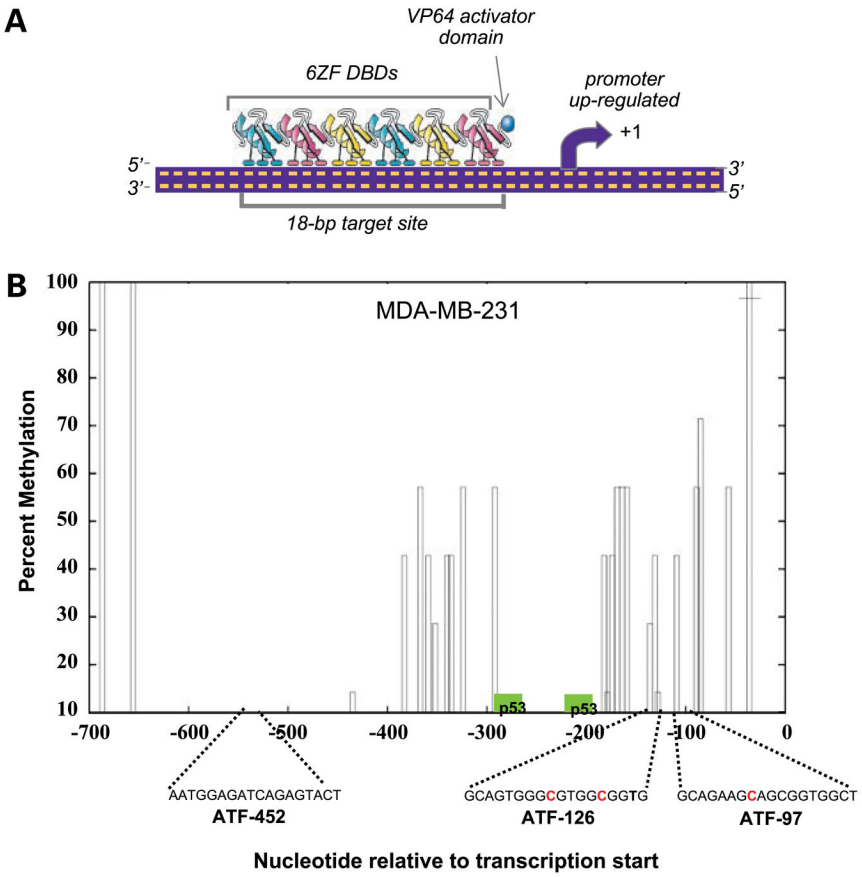

Figure 1.

ATFs designed to reactivate the *maspin* promoter. **A,** schematic representation of a 6ZF-ATF. **B,** cytosine methylation status of *maspin* in MDA-MB-231 breast cancer cells. *X axis,* nucleotide position relative to the transcription start site; *Y axis,* percentage of methylation along the *maspin* promoter. The *maspin* proximal promoter region (−495 to +134) was originally reported by Zhang et al. (53). 5-Methylcytosine levels were obtained by sodium bisulfite genomic sequencing of the *maspin* promoter from genomic DNA of untransduced MDA-MB-231 cells. Transcription factor–binding sites were included [p53-binding sites (35) and ATF-binding sites (27)]. Red nucleotides indicate the methylated cytosines in the ATF-binding sites.

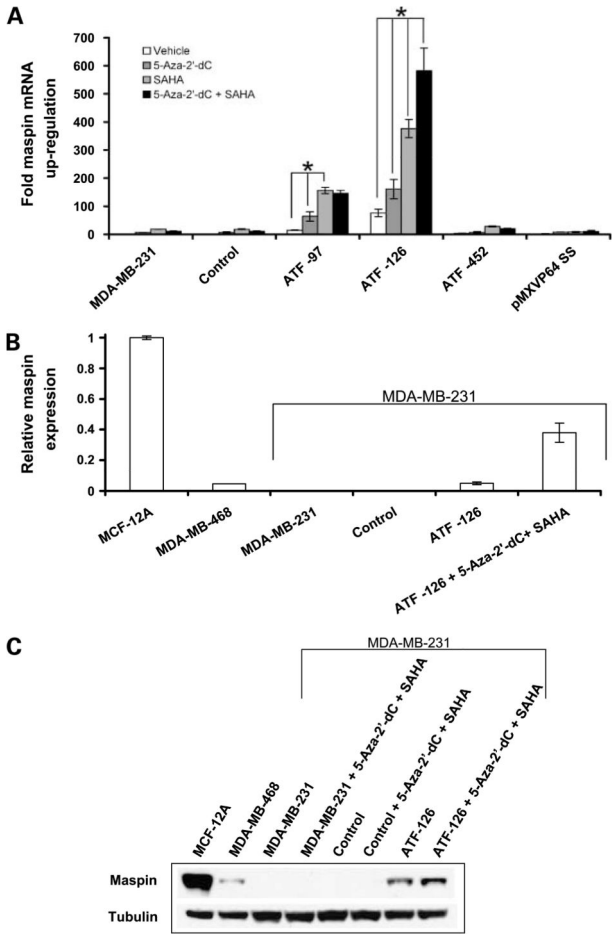

Figure 2.

ATFs synergize with chromatin remodeling drugs to reactivate *maspin* expression. **A,** real-time quantification of *maspin* in untransduced MDA-MB-231 cells, cells retrovirally transduced with an empty retroviral vector (control), cells transduced with ATFs, and cells transduced with a control retrovirus lacking the ZF domains (pMXVP64SS). These samples were treated with 5-aza-2′-dC (1.0 μg/mL) or SAHA (0.5 μg/mL) or both inhibitors (same concentrations) using complete cell culture medium for the dilution of the drugs during 48 h in a 37°C, 5% CO_2 incubator. Cells were collected, and the RNA was extracted, reverse transcribed, and processed for real-time *maspin* quantification. Real-time PCR data were analyzed using the comparative $2^{-\Delta\Delta CT}$ method and expressed as fold change in *maspin* mRNA expression normalized to *GAPDH* and relative to the vehicle-treated control (52). Differences between treatments were analyzed using ANOVA test and the post hoc Turkish test; critical level of significance was set up at $P < 0.05$. **B,** real-time expression analysis of *maspin* mRNA levels in the breast cancer cell lines MCF-12A, MDA-MB-468, and MDA-MB-231. MDA-MB-231 cells were transduced with a control empty retroviral vector, with ATF-126, and with ATF-126 in the presence of 5-aza-2′-dC (1.0 μg/mL) and SAHA (0.5 μg/mL). MCF-12A was used as a normalizing control. **C,** Western blot for the detection of maspin in the MCF-12A, MDA-MB-468, and MDA-MB-231 cell lines. MDA-MB-231 cells

were transduced with control vector or ATF-126 and treated with a combination of 5-aza-2′-dC/SAHA (0.5 and 1 μg/mL, respectively).

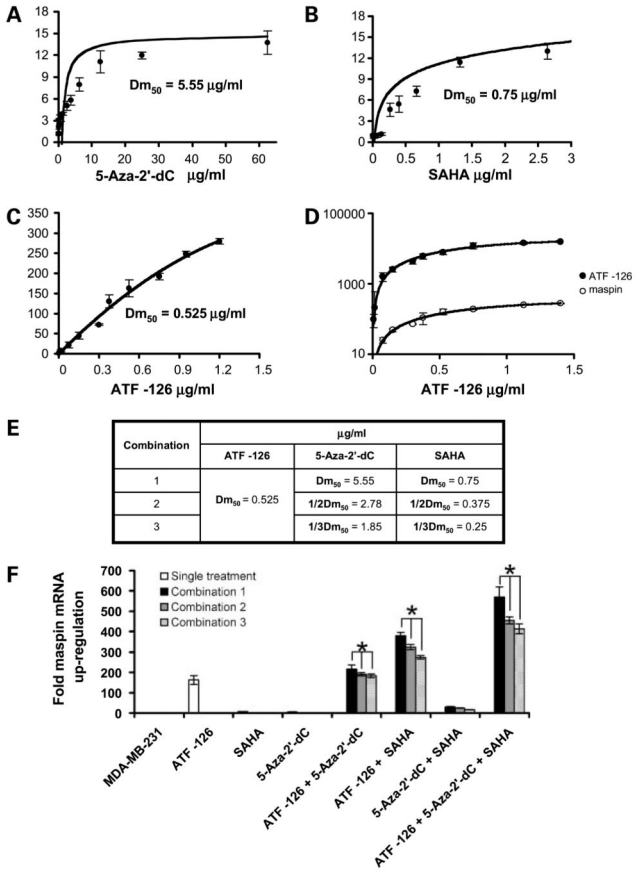

Figure 3.

ATFs synergize with low concentrations of chromatin remodeling drugs to reactivate *maspin* mRNA expression. **A** and **B,** dose-effect plots assessing changes in *maspin* mRNA levels in cells treated with different concentrations of 5-aza-2′-dC and SAHA. Fold *maspin* mRNA levels were evaluated by real-time PCR using as a normalized control vehicle-treated cells. **C,** dose-effect plots assessing changes in *maspin* mRNA levels in cells transduced with different concentrations of ATF-126. **D,** mRNA expression changes of ATF directly correlate with changes on *maspin* mRNA levels, as evaluated by real-time PCR using primers specific for the ATF and *maspin*, respectively. Changes in mRNA expression of the ATF were generated, varying the amount of ATF-encoded DNA in the retroviral transduction. **E,** concentrations of ATF, 5-aza-2′-dC, and SAHA used in each combination tested. **F,** real-time expression analysis of *maspin* mRNA expression in ATF-transduced cells treated with specific combinations of 5-aza-2′-dC, SAHA, and both inhibitors, as indicated in **E**. MDA-MB-231 cells were transduced with ATF-126 (0.525 µg/mL; the Dm_{50} for *maspin* expression) and treated with three different concentrations (Dm_{50}, $_{1/2}Dm_{50}$, and $_{1/3}Dm_{50}$) of either 5-aza-2′-dC, SAHA, or both compounds. Cells were collected, and the RNA was extracted, reverse transcribed, and processed for real-time quantification of *maspin*. Using fold change in *maspin*, mRNA expression was calculated using the comparative $2^{-\Delta\Delta C\ T}$ method as described above (52). Differences between treatments were analyzed using ANOVA test and the post hoc Turkish test; critical level of significance was set up at $P < 0.05$.

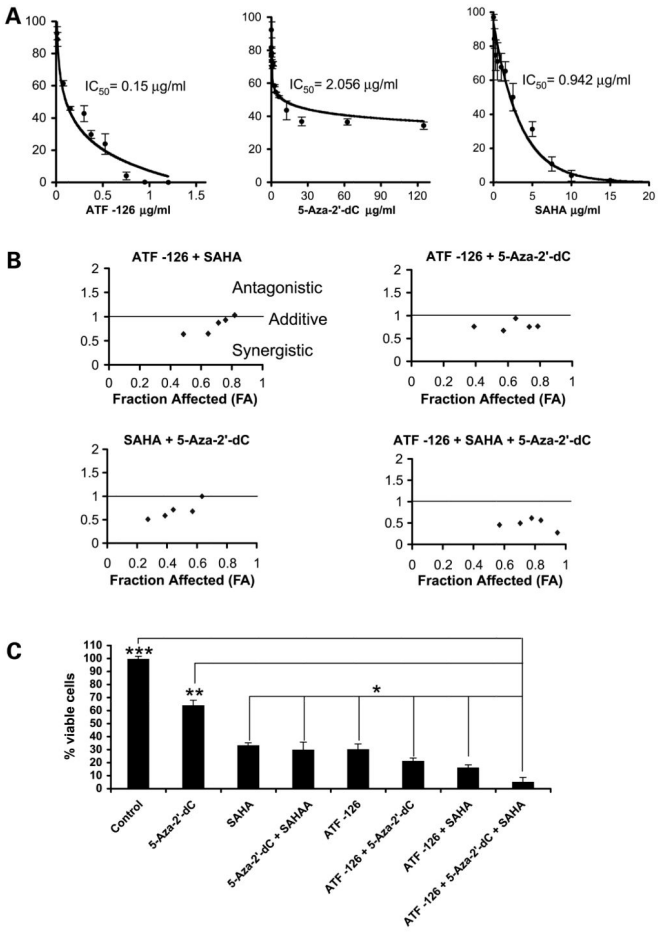

Figure 4.

ATF-126 synergizes with 5-aza-2′-dC and SAHA in inhibiting tumor cell viability. **A,** ATF-126, 5-aza-2′-dC, and SAHA induce inhibition of tumor cell viability in a dose-dependent manner. Dose-effect curves for cells transduced with different concentrations of the DNA of ATF-126 or treated with different concentrations of 5-aza-2′-dC and SAHA (Table 1).[3] The effects of the ATFs and the chromatin remodeling drugs in inhibiting tumor cell viability were measured by the ability of metabolic active cells to reduce the tetrazolium salt XTT to orange-colored compounds of formazan. Dose-effect curves and median-effect plots were generated for each set of samples using the software package PharmToolsPro (28). **B,** CI for cells transduced with ATF-126 and treated with 5-aza-2′-dC (ATF-126 + 5-aza-2′-dC), SAHA (ATF-126 + SAHA), and both inhibitors (ATF-126 + 5-aza-2′-dC + SAHA). Nontransduced cells were treated with both inhibitors (5-aza-2′-dC + SAHA). CI was calculated from the median-effect plots (31) to measure the synergistic action between ATF-126, 5-aza-2′-dC, and SAHA in the MDA-MB-231 breast cancer cell line. CI < 1 defines a synergistic interaction, and CI > 1 defines an antagonistic drug interaction. The straight line at CI = 1 represents additive effects. **C,** inhibition of tumor cell viability on ATF-126 transduction and/or treatment with chromatin remodeling drugs. For single treatments, MDA-MB-231 cells were transduced with ATF-126 (0.525 µg/mL) or treated with 5-aza-2′-dC (3.75 µg/mL) and SAHA (1.32 µg/mL) for 48 h at 37°C and 5% CO_2. The

same concentrations were used for the following combinations: 5-aza-2′-dC + SAHA, ATF-126 + 5-aza-2′-dC, ATF-126 + SAHA, and ATF-126 + 5-aza-2′-dC + SAHA. Cell viability was measured using the XTT assay, as described above. The data were analyzed using an ANOVA test and a post hoc Turkish test, as described in Materials and Methods. The asterisks indicate that the triple treatment decreased significantly tumor cell viability compared with all the other treatments tested. *, $P = 0.05$; **, $P = 0.01$; ***, $P = 0.001$.

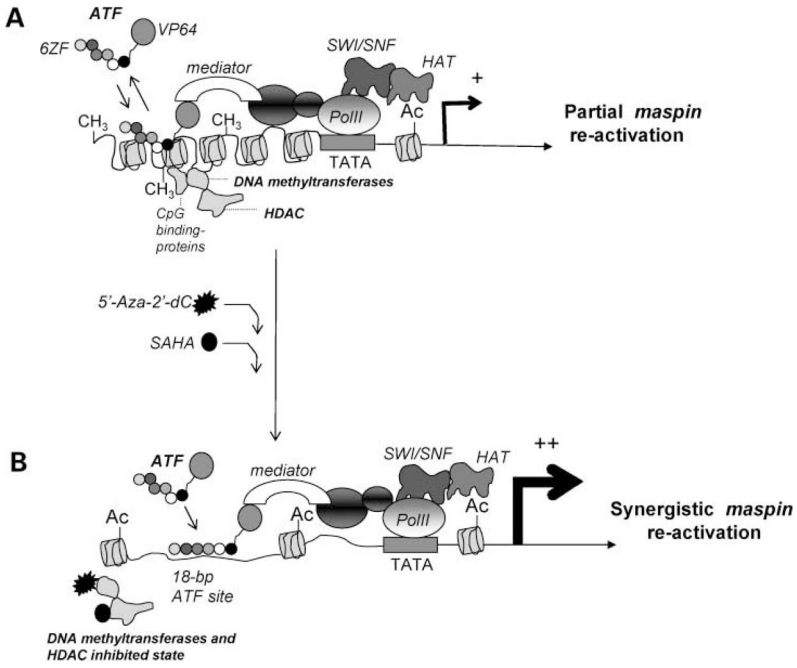

Figure 5.

A putative model explaining the synergy between the ATF and the chromatin remodeling drugs in reactivating a methylated *maspin* promoter. **A,** the binding of ATF to the methylated promoter triggers a partial reactivation of the *maspin* gene. **B,** synergistic interaction between the ATFs and chromatin remodeling drugs. On treatment with chromatin remodeling drugs, changes in the chromatin structure facilitate the landing of ATF on the *maspin* promoter, which enhances the *maspin* reactivation.

Table 1

CI values for single, double, and triple combinations of ATF-126, 5-aza-2′-dC, and SAHA

ATF/Drug (μg/mL)			fa	CI
ATF-126	SAHA	5-aza-2′-dC		
0.075	0.13215		0.484	0.633
0.150	0.264		0.645	0.647
0.300	0.396		0.713	0.874
0.375	0.661		0.758	0.930
0.525	1.322		0.819	1.028
0.075		0.250	0.389	0.763
0.150		0.625	0.571	0.673
0.300		1.250	0.648	0.939
0.375		2.500	0.733	0.755
0.525		3.750	0.786	0.767
	0.132	0.250	0.272	0.507
	0.264	0.625	0.386	0.583
	0.396	1.250	0.441	0.712
	0.661	2.500	0.570	0.675
	1.322	3.750	0.634	1.000
0.075	0.132	0.250	0.569	0.456
0.150	0.264	0.625	0.704	0.497
0.300	0.396	1.250	0.779	0.613
0.375	0.661	2.500	0.839	0.561
0.525	1.322	3.750	0.947	0.275

NOTE: Experimental dose combinations of ATF-126, SAHA, and 5-aza-2′-dC are indicated. MDA-MB-231 cells were transduced with ATF-126 and treated with 5-aza-2′-CC or SAHA or both for 48 h. Cell viability was measured by using an XTT assay.

Abbreviation: fa, fraction of cells affected by the treatment (no viable cells).